ICFM 10
Adapting to Global Change:
Innovative Approaches to Flood Management and Resilience
May 20-22, 2026 | Western University, London, Ontario, Canada

Research on Improving the Accuracy of Flood Prediction Technology Using Satellites, Drones and Digital Testbeds

Tetsuya Takeshita[1], Hisashi Kuronuma[1], Yuki Hamada[1], and Yoshimasa Morooka[1]
National Institute for Land and Infrastructure Management (NILIM),
Ministry of Land, Infrastructure, Transport and Tourism (MLIT),
1, Asahi, Tsukuba, Ibaraki, 305-0804, Japan[1]
E-mail: takeshita-t2hp@mlit.go.jp

ABSTRACT

In response to the frequent occurrence of flood damage, NILIM developed a river-water-level prediction system for Japan. This system has been operational since 2020. The system uses actual and predicted rainfall data as input conditions and predicts river water levels 6 hours ahead at 200-meter intervals. In addition, the accuracy of flood forecasting is improved by assimilating observed water levels from several water level stations in rivers with calculated water levels through data assimilation using particle filters. However, it is difficult to confirm or improve the prediction accuracy of the longitudinal water level of rivers between water level stations because there are no observation data.

Therefore, NILIM has developed 1) a method for grasping the longitudinal water level of the river using satellites with synthetic aperture radar (SAR), 2) a method for correcting observed data by SAR satellites using a water-landing drone equipped with the real-time kinematic global navigation satellite system (RTK-GNSS) and a microwave reflector, and 3) digital testbeds for water level estimation using SAR satellites and flood prediction accuracy evaluation.

The mean absolute errors of the estimated water levels using SAR satellites were 0.35-1.42 m. As a result of a demonstration experiment in the Nikko River, the mean absolute error of water levels was 0.03 m, measured by the water-landing drone and the fixed water-level station, and the trajectory of the drone was confirmed from a SAR satellite image. In addition, NILIM has developed a water-level estimation tool for SAR satellites and an accuracy evaluation tool for flood prediction on digital testbeds, which are experimental sites in a cloud environment.

KEYWORDS: Flood prediction, SAR satellites, drones, digital testbed, accuracy evaluation

1 INTRODUCTION

In response to the recognition of the importance of prediction information in Japan, which was triggered by Hurricane Sandy in the United States in 2012 and torrential rains in the Kanto and Tohoku regions in 2015, NILIM started to develop a flood risk line, a national river water level prediction system, in fiscal 2014. The system has been in operation since 2020 (Web-1) and is currently used for the flood forecasting. Tsuchiya et al. (2023) have described this in detail. The system calculates river water levels 6 hours ahead at 200 m intervals by combining the runoff analysis model and the river channel analysis model with the input conditions of actual rainfall data by radar and predicted rainfall data by the Japan Meteorological Agency. In addition, Tachikawa et al. (2011) attempted to improve flood prediction accuracy by assimilating the observed water level data from several water level observation stations in the target river with the calculated water level using particle filters. The parameters to be filtered by particle

filters are the storage volume of the runoff model and the roughness coefficient of the river channel model.

However, it is difficult to confirm and improve the prediction accuracy of the longitudinal water level of the river between water level observation stations because there are no observation data of the longitudinal water level in the section between the water level observation stations. In addition, the length of Class A rivers managed by the national government is 10,671 km, and it is expensive to install conventional fixed water level observation stations at intervals of 200 m to 1 km to grasp the longitudinal water level.

Therefore, in this study, we first developed an estimation method for river water levels using SAR satellites, which can observe over a wide area at night and under bad weather conditions. Second, to correct the observation error caused by the spatial resolution of SAR satellite data, we examined a correction method for the estimated water level using a joint observation between the SAR satellite and a water-landing drone equipped with a real-time kinematic global navigation satellite system (RTK-GNSS) and a microwave reflector. Third, we developed a water-level estimation tool for SAR satellites and an accuracy evaluation tool for flood prediction on digital testbeds, which are experimental sites in a cloud environment.

2 DEVELOPMENT OF ESTIMATION METHOD OF RIVER WATER LEVELS USING SAR SATELLITES

SAR satellites irradiate L-band or X-band microwaves and measure the intensity of back reflection. It is possible to observe over a wide area at night and under adverse weather conditions. Recently, small SAR satellite constellations have been developed, and observation frequencies have been improved. Regarding the estimation method of river water level using SAR satellites, Biondi et al. (2019) and Chen et al. (2021) estimated the water level near a bridge using the multiple bounce scattering phenomenon of the bridge. However, it is necessary to estimate the water level other than near the bridge to estimate the longitudinal water level of the river.

Therefore, in this study, as shown in Figure 1, we interpreted the position of the waterline from the SAR satellite data and estimated the water level of the water edge line from the point cloud data of the topography. The specific methods, results, and discussion are presented below.

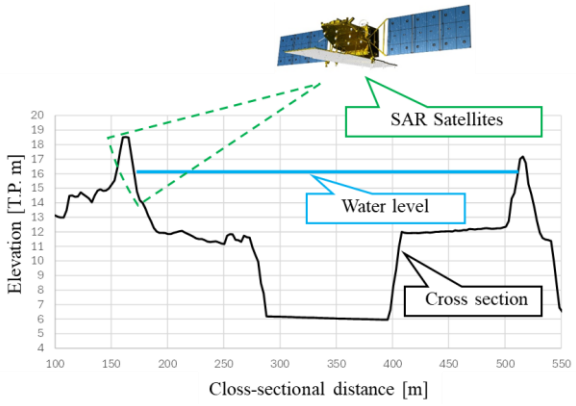

Figure 1: Image of river water level estimation by SAR satellites

2.1 Estimation method of river water level

The procedure for estimating river water levels using SAR satellites is shown below.

1) Preprocessing of SAR satellite images

The SAR satellite images were GEO-TIFF files of product level 2.1, which were converted to orthographic images using ortho-correction. Multiple representative points, such as bridges, were defined as Ground Control Points (GCPs) from the 3D point cloud data of the topography, and the SAR satellite images were geometrically corrected so that the positions of the GCPs in the topography data matched. In addition, filter processing was performed to reduce the speckle noise specific to SAR satellite images. In this study, a Frost filter (Frost et al. (1982)) with a filter window size of 5×5 was used.

2) Creating images near water edge

Because SAR satellites irradiate microwaves in the oblique direction, the backscatter on the water surface is small owing to specular reflection and appears black in SAR satellite images. Therefore, as shown in Figure 2, we extracted digital numbers (integer value with a minimum of 0 and a maximum of $2^{16} = 65536$) of backscatter intensity at several hundred points at the center line of the river, assumed a normal distribution of backscatter intensity in the water area, and binarized the water and land area with a threshold value of $+\sigma$ from the average value. Considering that the water area is underestimated by the average value, we set a threshold value of 84% from the smallest backscatter intensity at the center line of the river.

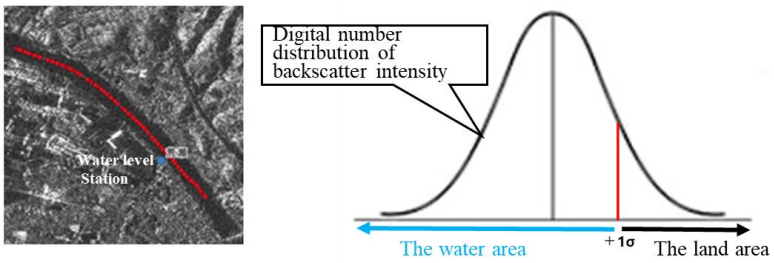

Figure 2: Approach to setting a threshold value for water edge positioning

3) Estimating water levels at water edge lines

As shown in Figure 3, 3D topographic images were displayed on GIS (using Arc GIS) based on topographic point cloud data and aerial photographs, and elevation lines parallel to levee normal lines were displayed at intervals of 2.5 m in the plane width. We then estimated the water levels by overlaying the elevation parallel lines and SAR images near the water edge created in 2) above. For locations where SAR images at two different time points of flood and normal were available, the differences in pixel values between the two time points were also output.

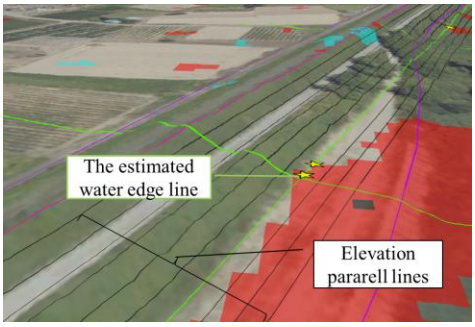

Figure 3: Water level estimation at water edge lines

2.2 Results

Table 1 shows the results of the water level estimation using L-band (ALOS -2, Web-2) and X-band (Strix, Web-3) SAR satellite images.

We calculated the mean absolute error between the estimated water levels using SAR satellites and the longitudinal water levels extrapolated from the observed water levels at water level observation

stations by the longitudinal slopes of the river (slopes of levee normal lines). The mean absolute errors for each type of SAR image and processing condition were between 0.35 and 1.42 m.

Table 1 Results of the estimated water levels using the SAR satellites

Microwaves	Single image or Two images	Mode	Spatial Resolution /Range Azimuth	Number of target points	Mean absolute error (m)
L-band	Two images	Strip map	3m / 3m	6	0.35
L-band	Single image	Strip map	3m / 3m	6	1.42
X-band	Single image	Strip map	3.6m / 2.6m	5	0.51

2.3 Discussion

As shown in Table 1, the estimation method of river water level using only SAR satellites does not have sufficient accuracy to be used as the observation value of the longitudinal river water level. This is due to the limitation of the spatial resolution of satellite data and the use of the mean value and standard deviation of digital numbers of the backscatter intensity of streamlines to set the threshold value for determining the water and land areas.

In the L-band, the mean absolute errors using two images were smaller than those using a single image. This is because it was easier to grasp the position of the waterline by adding the information of the difference using two images. In addition, the mean absolute errors were smaller in the X-band than in the L-band using a single image. This is due to the difference in spatial resolution. In the future, as the number of observation images by SAR satellites increases owing to the development of small SAR satellite constellations, it will be possible to estimate water levels using the X-band difference using two images, and it is expected that the mean absolute errors will be smaller than those obtained using single images. It is also possible to further reduce the mean absolute errors in the L-band by revising the threshold of the water edge position. In particular, the L-band satellite ALOS2 has an observation width of 50 km at a spatial resolution of 3 m, which is wider than the X-band satellite Strix, which has an observation width of 30 km. The advantage is that it is easy to estimate water levels using two images because some images already exist in the dataset.

3 EXAMINATION OF A CORRECTION METHOD FOR ESTIMATED WATER LEVELS BY JOINT OBSERVATION WITH A DRONE AND A SAR SATELLITE

As described in 2., the estimation method of river water levels using only the SAR satellite does not have sufficient accuracy to be used as the observation value of the longitudinal water levels of the river. To improve the estimation accuracy of river water levels, it is necessary to improve the threshold setting of the binarization judgment of the water and land areas using satellite data and the method of water level estimation at the water's edge.

Therefore, in this study, we examined a technology to correct the estimated water level by linking the observation of water levels at the site using a water-landing drone and observation using a SAR satellite. The details are described below.

3.1 Observation method

On February 23, 2025, we conducted water level observations at the mouth of the Nikko River in Aichi Prefecture, Japan (Figure 4), using a landing downstream drone and a SAR satellite. The SAR satellite used Strix to observe an area of approximately 3 km and 10 km, as indicated by the red frame in Fig. 4 in the Staring Spotlight mode. The landing downstream drone (Web-4) is under development by SBIR (Small/Startup Business Innovation Research), a system to promote the R&D of Japanese start-up companies. As shown in Figure 5, it is equipped with a propeller for flight, a self-propelled screw on

water, and an RTK-GNSS positioning function for water-level observation. It is also equipped with a microwave reflector for observations. The river survey method using a SAR satellite and a water-landing drone has been patented by NILIM.

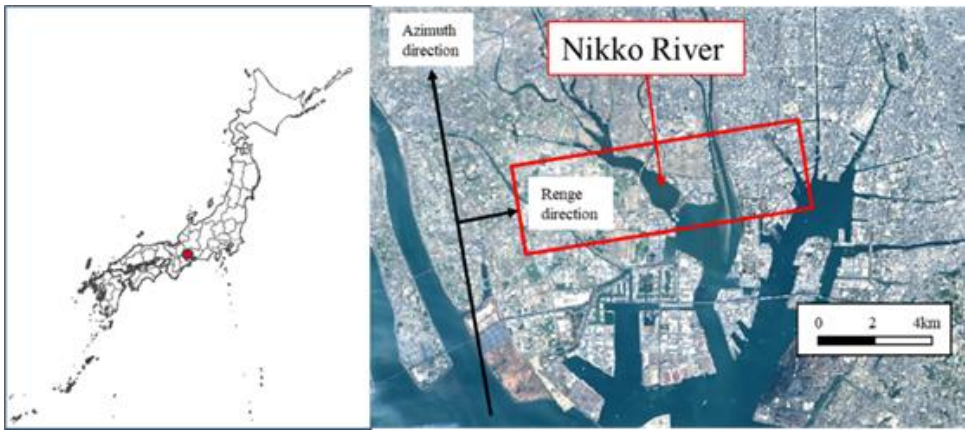

Figure 4: Observation location map (Nikko River)
(Source: partly modified from Geographical Survey Institute map)

Figure 5: Pictures of a water-landing drone (left: before landing, right: after landing)

3.2 Results

The observation results from 15:14 8.8 s to 15.1 s (6.3 s) on February 23, 2025, are shown in Figure 6 and Table 2. As shown in Figure 6, the SAR satellite image confirmed the position of the water-landing drone. In the staring spotlight mode, the SAR satellite fixed the observation range in the red frame in Figure 4 and observed while moving; thus, the movement of the drone under the landing stream was captured as a trajectory. The actual trajectory of the drone and the extension of the trajectory in the SAR satellite image were displayed differently owing to the scattering of microwaves.

Table 2 shows the results of comparing the water level estimated only by the SAR satellite and the water level observed by the water-landing drone with that observed by the fixed water-level observation station at the mouth of the Nikko River.

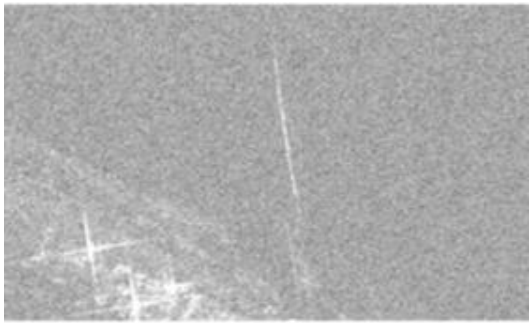

Figure 6: a trajectory of the drone confirmed by the SAR image

Table 2 Comparison results of water level for each observation and estimation method

Observation and estimation method	(a) An observed water level at a fixed water level station	(b) An estimated water level using only a SAR image	(c) An observed water level using a water-landing drone
Water level	T.P. - 0.39 m	T.P. 1.00 m ((b) - (a) = 1.39m)	T.P. -0.43 m (30 second average) ((c) - (a) = - 0.04m) Fluctuation range of instantaneous value T.P.-0.51m ~ -0.35m

T.P. (Tokyo Peil): mean sea level of Tokyo Bay

3.3 Discussion

As shown in Table 2, the water level estimated only by the SAR satellite was 1.39 m higher than that observed by the fixed water level observation station. This is because the wind was slightly strong at the time of the observation (Nagoya observation station: average wind speed 4.4 m/s at 15:10 on February 23, 2025). The fluctuation range of the instantaneous value of the water level observed by the drone below the landing stream also indicated that the water surface fluctuated. Therefore, it is highly probable that the back-reflection intensity was affected by fluctuations in the water surface.

In contrast, the 30 s average water level observed by the drone, as shown in Table 2, had an error of 0.04 m compared with the water level at the fixed water level station, indicating good observation accuracy. It was expected that the drone could observe the water level at any point as a mobile water level gauge and use it as data to correct the water level estimated by the SAR satellite.

In this way, the drone can observe the water level fluctuation and the water level at any point. As shown in Figure 6, the position of the drone can also be identified from SAR satellite images. Therefore, it is expected that the observation data by the drone could be used to set the threshold value of the back reflection intensity (pixel value) and to correct the estimated water level to improve the accuracy of discrimination between water and land areas by SAR images.

4 DEVELOPMENT OF FLOOD FORECASTING ACCURACY EVALUATION TOOL USING DIGITAL TESTBEDS

The Water and Disaster Management Bureau (WDMB) of MLIT is developing a watershed data platform (Hereinafter referred to as DPF), which standardizes the data format and enables automatic updating of watershed data in 109 class A river systems managed by the national government. The DPF is an information infrastructure in a cloud environment, and watershed data, such as 3D topographic point cloud data can be utilized.

Therefore, NILIM, in cooperation with WDMB, developed Digital Testbeds (Hereinafter referred to as DTB) in the DPF as watershed experiment sites in cyberspace that can utilize DPF data (Takeshita et al. (2025)) and started trial use of the DTB in October 2025. As part of the trial use of the DTB, NILIM is using the DTB to visualize rivers in 3D, as shown in Figure 3, and is using it for research on water level estimation by SAR satellites. In addition, an accuracy evaluation tool is under development to verify the prediction accuracy of flood risk lines, in the national flood prediction system.

The display screen of the accuracy evaluation tool is shown in Figure 7, and the main evaluation indices are listed in Table 3. The equations for the Nash-Sutcliffe coefficient and error evaluation index "*E*" are shown in Equations (1), (2) and (3). By utilizing watershed data, visualization tools and accuracy evaluation tools on DTB, we will verify the accuracy of flood risk line prediction in the country and promote R&D to improve the accuracy of flood prediction through public-private collaboration.

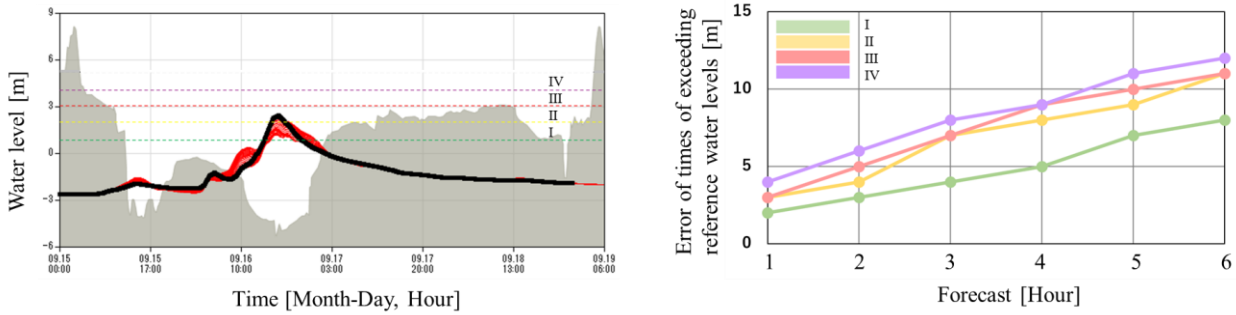

Figure 7: Screen display images of the flood prediction accuracy evaluation tool

Table 3 Evaluation indices of the flood prediction accuracy evaluation tool

Evaluation objects	Evaluation indices
Water levels	Error of peak water level, Error rate (=Error / peak water level)
	Error of reference water levels (I to IV), Error rates (=Errors /reference water levels) I: Reference water levels for flood-fighting corps to begin standby II: Reference water levels for flood-fighting corps to begin activities III: Reference water levels for evacuation of the elderly people, etc. IV: Reference water levels for evacuation instruction
Times	Error of peak water level times
	Error of times of exceeding reference water levels (I to IV)
Water-level hydrographs	RMSE (Root Mean Square Error)
	Nash-Sutcliffe (*NS*) coefficient (Equations (1) and (2))
	Error evaluation index "*E*" (Equation (3))

$$NS = 1 - \frac{\sum_{i=1}^{N}\{h_o(i)-h_c(i)\}^2}{\sum_{i-,}^{N}\{h_o(i)-h_{av}\}^2} \quad (1)$$

$$h_{av} = \frac{1}{N}\sum_{i=1}^{N} h_o(i) \quad (2)$$

$$E = \frac{1}{N}\sum_{i=1}^{N}\left\{\frac{h_o(i)-h_c(i)}{h_{op}}\right\}^2 \quad (3)$$

N: calculation times, $h_o(i)$: measured water levels at time i, $h_c(i)$: calculated water levels at time i, h_{av}: measured average water levels, h_{op}: measured peak water levels

5 CONCLUSIONS

The conclusions of this study are as follows.

1) We developed a river water level estimation method using SAR satellites and compared the measured water level with the estimated water level using SAR satellites. The mean absolute errors were between 0.35 m and 1.42 m for each type of SAR image and processing condition.
2) As a result of carrying out the observation of the Nikko River in cooperation with a SAR satellite and a water-landing drone equipped with an RTK-GNSS positioning function and a microwave reflector, the error of the water level observed by the fixed water level observation station and the water-landing drone was 0.04 m, and the trajectory of the drone was confirmed from the SAR satellite image. This result is expected to be useful for correcting the water level estimated by the SAR satellite based on the water level observed by the drone and for improving the accuracy of discrimination between water and land areas.
3) Using the digital testbed, we conducted research on water-level estimation using SAR satellites and are developing an accuracy evaluation tool for flood forecasting. In the future, we plan to use this tool for research and development to verify and improve the accuracy of the national flood forecasting system.

6 ACKNOWLEDGEMENTS

The authors would like to express their sincere gratitude to WDMB of MLIT, Pacific Consultants Co., Ltd., Remote Sensing Technology Center of Japan, Prodrone Co., Ltd., Synspective Inc., Japan Aerospace Exploration Agency and CTI Engineering Co., Ltd. for their cooperation in this research.

This research was also supported in part by the research budget of BRIDGE (Programs for bridging the gap between R&D and the ideal society (society 5.0) and generating economic and social value). We would like to express our gratitude.

REFERENCES

Biondi, F., Tarpanelli, A., Addabbo, P., Clemente, C. and Orlando, D. (2019). Pixel tracking to estimate rivers water flow elevation using Cosmo SkyMed synthetic aperture radar data, Remote Sensing 11 (21), 2574.

Chen, X., Zheng, Y., Peng, J. and Floris, M. (2021). Monitoring river water level using multiple bounces of bridges in SAR images, Advances in Space Research 68, pp.4016-4023.

Frost, V. S., Stiles, J. A., Shanmugan, K. S. and Holtzman, J. C. (1982). A model for radar images and its application to adaptive digital filtering of multiplicative noise, IEEE Trans. Pattern Analysis and Machine Intelligence, Vol.4, No.2, pp.157-166.

Tachikawa, Y., Sudo, J., Shiiba, M., Yorozu, K. and Kim, S. (2011). Development of A Real-Time River Stage Forecasting Method using a Particle Filter, Journal of JSCE, B1, Vol.67, No.4, pp. I_511-I_516.

Takeshita, T., Morooka, Y., Yamaji, H., Kuronuma, H., Ozawa, K., Hamada, Y. (2025). Development of Digital Testbeds to Support the Policy of River Basin Disaster Resilience and Sustainability by All, Proceedings of the 41st IAHR World Congress, pp.1001-1008, Singapore, June 22-27.

Tsuchiya, S., Morooka, Y. and Takeshita, T. (2023). Development of the river water level prediction method using data assimilation and the display system called Flood Risk Line, Extended Abstracts of the 9th International Conference on Flood Management, No.19-03, Tsukuba, Ibaraki, Japan, February 18-22.

Web sites:

Web-1: https://frl.river.go.jp, consulted 29 November 2025.

Web-2: https://www.eorc.jaxa.jp/ALOS/en/alos-2/datause/a2_format_e.htm, consulted 29 November 2025.

Web-3: https://synspective.com/document/, consulted 29 November 2025.

Web-4: https://sbir.csti-startup-policy.go.jp/phase3fund, consulted 29 November 2025.

(SBIR Demonstration Project Compendium (Ver.2).pdf, p.124)